LANGMUIR

Article

pubs.acs.org/Langmuir

High-Throughput Screening of Metal−Organic Frameworks for CO_2 Capture in the Presence of Water

Song Li,[†] Yongchul G. Chung,[‡,§] and Randall Q. Snurr*[,‡]

[†]State Key Laboratory of Coal Combustion, School of Energy and Power Engineering, Huazhong University of Science and Technology, Wuhan 430074, China

[‡]Department of Chemical and Biological Engineering, Northwestern University, Evanston, Illinois 60208, United States

[§]School of Chemical and Biomolecular Engineering, Pusan National University, Busan 609-735, Korea (South)

ABSTRACT: Competitive coadsorption of water is a major problem in the deployment of adsorption-based CO_2 capture. Water molecules may compete for adsorption sites, reducing the capacity of the material, and dehumidification prior to separating CO_2 from N_2 increases process complexity and cost. The development of adsorbent materials that can selectively adsorb CO_2 in the presence of water would be a major step forward in the deployment of CO_2 capture materials in practice. In this study, large-scale computational screening was carried out to search for metal−organic frameworks (MOFs) with high selectivity toward CO_2 over H_2O. Calculating framework charges for thousands of MOFs is a significant challenge, so initial screening used a fast, but approximate, charge calculation method. On the basis of the initial screening, 15 MOFs were selected, and Monte Carlo simulations were carried out to compute the adsorption isotherms for these MOFs using more accurate framework charges calculated by density functional theory. A detailed investigation was performed on the effect of using different methods for calculating partial charges, and it was found that electrostatic interactions contribute the majority of the adsorption energy of H_2O in the selected MOFs.

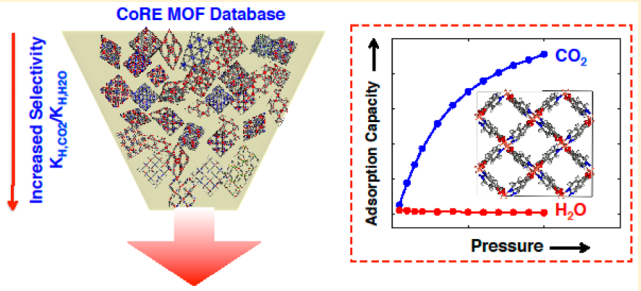

1. INTRODUCTION

Our climate is rapidly changing due to increased emissions of CO_2 to the atmosphere from fossil-fuel-burning power plants.[1,2] To mitigate drastic changes to our atmosphere, several carbon capture and sequestration (CCS) strategies have been developed, such as amine-containing solvent absorption[3] and membrane separation,[4] and some of these methods are now being deployed on small scales. In addition, recent years have seen a surge of industrial and academic interest in CCS strategies based on solid adsorbents as an attractive, energy-saving alternative.[4−6] The key challenge in adsorbent-based CO_2 capture, however, is to find a suitable, high-performing adsorbent material that can selectively adsorb CO_2 over other gas molecules, such as nitrogen and water.

A wide range of materials, such as zeolites, activated carbons, silica, and metal−organic frameworks (MOFs),[7,8] have been tested for selective adsorption of CO_2 at the laboratory scale. MOFs are crystalline microporous materials formed by self-assembly of organic struts and inorganic metal nodes. Because of their unique physical characteristics, such as ultrahigh surface area, high porosity, and tunable chemical properties,[4,9] MOFs have been regarded as a particularly promising class of adsorbent material for postcombustion carbon capture,[5,10−13] and there are a large number of studies that report selective adsorption of CO_2 over N_2 in MOFs. However, postcombustion carbon capture using adsorbents must also address the presence of water vapor in the flue gas stream, because the presence of water can adversely affect the adsorption of CO_2 and N_2 by competing for adsorption sites and by affecting MOF stability.[14−17] We do not address MOF stability issues in this paper, but we explore the hypothesis that MOFs exhibiting little or no adsorption of water (i.e., hydrophobic MOFs) might be promising candidates for carbon capture. The key structural characteristics that are responsible for creating hydrophobic behavior are not well understood although the links between molecular properties and the hydrophobicity of MOFs are beginning to emerge.[18,19] An advantage of adopting hydrophobic MOFs for CO_2 capture is that the cost of removing water from the flue gas could be avoided[20] and water could be easily removed from the CO_2 product during the process of compressing it for pipeline transport.

In the literature, more than 5000 MOFs have been reported to date, and it is clearly not possible to test the performance of all of these materials for postcombustion CO_2 capture, considering the time and cost associated with MOF synthesis, activation, and testing. As an alternative, we adopt a high-throughput computational screening strategy to identify high-performing MOFs for postcombustion CO_2 capture under the presence of water vapor from a large number of structures.[21] Such methods have been successfully employed in the

Received: July 27, 2016
Revised: September 10, 2016
Published: September 14, 2016

DOI: 10.1021/acs.langmuir.6b02803
Langmuir 2016, 32, 10368−10376

discovery of MOF candidates for hydrogen storage,[22,23] Xe/Kr separation,[24] ethanol/water separation,[25] and methane storage and delivery.[26] In addition, there have been several reports focused on identifying promising materials for CO_2 capture via computational screening.[10,27,28]

In this work, we aim to identify MOFs with high CO_2 selectivity under high humidity conditions (RH = 80%) via high-throughput grand canonical Monte Carlo (GCMC) simulations of existing MOF structures[29] and to provide some guidelines regarding different methods for estimating the partial charges of MOF atoms for large-scale screening, especially for adsorption of polar molecules such as water. Prediction of water adsorption in MOFs with GCMC is very time-consuming. To avoid such time-consuming simulations for thousands of candidate structures but simultaneously to identify MOFs that can selectively adsorb CO_2 over water, we first used the ratio of Henry's law constants between CO_2 and H_2O to identify high-performing MOFs. On the basis of this initial stage of screening, the 15 top MOFs were identified and GCMC simulations were carried out for these 15 materials to validate our approach.

For the Henry's constant calculations, the partial charges of framework atoms were obtained from the extended charge equilibration (EQeq) method.[30] Similar strategies have been successfully used for separation of CO_2/N_2[31,32] and ethanol separations.[25] However, we wondered if adsorption of a highly polar molecule, such as water, might be sensitive to the method used in calculating the MOF partial atomic charges. To investigate this question, the performance of the top-performing MOFs from the initial screening was re-evaluated with more accurate partial atomic charges derived from plane-wave density functional theory (DFT) calculations. Our results show that the electrostatic interaction plays a dominant role in determining the water adsorption behavior in MOFs and that a judicious decision must be made in choosing the method for calculating framework atomic charges.

2. COMPUTATIONAL METHODS

Model. A Lennard-Jones (LJ) plus Coulomb potential was used to describe the nonbonded interactions between atoms in the framework and the adsorbates

$$V_{ij} = 4\varepsilon_{ij}\left[\left(\frac{\sigma_{ij}}{r_{ij}}\right)^{12} - \left(\frac{\sigma_{ij}}{r_{ij}}\right)^{6}\right] + \frac{q_i q_j}{4\pi\epsilon_0 r_{ij}} \quad (1)$$

Here, i and j index the interacting atoms, r_{ij} is the distance between atoms i and j, q_i and q_j are the partial atomic charges on atoms i and j, ε and σ are the LJ parameters, and ε_0 is the vacuum permittivity constant. The ε and σ parameters for the framework atoms were taken from the universal force field (UFF),[33] which has been validated for high-throughput screening of MOFs by comparing with ab initio force fields.[34] The TraPPE force field[35] was used to model CO_2 and N_2, and the TIP4P[36] model was used for H_2O molecules. The TraPPE force field was designed to work well with TIP4P, so this is a consistent choice.[37] LJ parameters between different atom types were calculated using the Lorentz–Berthelot mixing rules. LJ interactions were cutoff at 12.8 Å, and each simulation cell was replicated in all directions to obey the minimum image convection with respect to this cutoff value. The long-range electrostatic interactions arising from the presence of atomic partial charges were summed using the method of Ewald.[38] The partial charges of framework atoms were obtained from the extended charge equilibration method (EQeq) with a default value of the dielectric strength (ε_R = 1.67).[30] All atoms in the MOFs were held fixed during the simulations.

Screening Procedure. Figure 1 summarizes the high-throughput computational screening procedure used in this study. The MOF

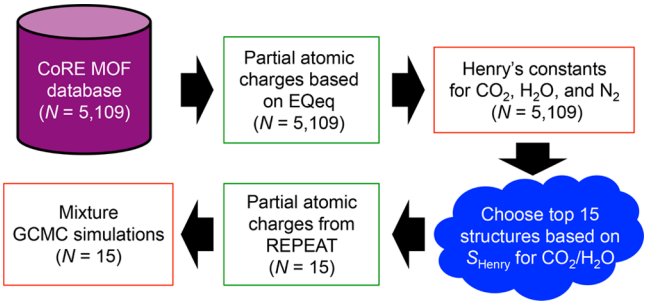

Figure 1. Workflow of the computational screening strategy employed in this study. N is the number of MOF structures involved in each step.

structures were taken from the computation-ready, experimental (CoRE) MOF database, where the free and coordinated solvent molecules were removed.[29] Partial charges on MOF atoms for the CoRE MOF structures were computed for all 5109 structures with the EQeq method, and the Henry's constants were calculated for these structures as described below. Among 5109 structures, MOFs with zero accessible surface area and structures with high adsorption energy of H_2O (>45 kJ/mol, which is larger than the heat of vaporization of the TIP4P model) were discarded from the set. The data from the remaining 2054 structures were used for further analysis. The ratio of the Henry's constants between CO_2 and H_2O

$$S_{\text{Henry}} = \frac{K_{\text{H,CO2}}}{K_{\text{H,H2O}}} \quad (2)$$

was used to select the 15 MOF structures with the highest estimated selectivity. Here, $K_{\text{H,CO2}}$ is the Henry's law constant of CO_2, and $K_{\text{H,H2O}}$ is the Henry's law constant of H_2O. The partial atomic charges of these 15 MOFs were recomputed using the Repeating Electrostatic Potential Extracted ATomic (REPEAT) method,[39] which computes the partial atomic charges by fitting to the electrostatic potential surface obtained from the electron densities within the periodic system obtained from plane-wave density functional theory (DFT) using the Vienna ab initio software package (VASP).[40−43] The DFT calculations were carried out based on the plane-wave method using the generalized gradient approximation (GGA) exchange-correlation functional and pseudopotential developed by Perdew, Burke, and Ernzernhof (PBE).[44] The electron−ion interaction was described by the projector augmented wave (PAW) scheme with an energy cutoff of 550 eV. A 1 × 1 × 1 Monkhorst−Pack k-point mesh was used for Brillouin zone sampling in the reciprocal space with spin polarization.

Grand Canonical Monte Carlo Simulations and Henry's Constant Calculations. GCMC simulations[45] were carried out to compute the binary and ternary adsorption of CO_2/H_2O and $CO_2/H_2O/N_2$ mixtures for the 15 MOFs identified in the initial screening. One million Monte Carlo cycles were performed to compute the adsorption properties of both binary and ternary mixtures. The first 50% of the cycles were spent on the equilibration, and the remaining cycles were used to compute the ensemble averages of properties of the system. For a cycle, N Monte Carlo moves were performed, selected from insertion, deletion, translation, rotation, and identity change of molecules with equal probability, where N is the number of adsorbates in the simulation box at the beginning of the cycle. If the system contains less than 20 adsorbates, 20 Monte Carlo moves were carried out for that cycle. For the ternary mixtures, the molar ratio of CO_2/N_2 was 1:9, and for both CO_2/H_2O and $CO_2/H_2O/N_2$ mixtures a relative humidity (RH) of 80% was used. To keep the relative humidity of the system constant, the partial pressure of H_2O was fixed at 3280 Pa, which is 80% of the vapor pressure of the TIP4P water model.[46] The selectivity from GCMC simulations was computed from the following definition:

DOI: 10.1021/acs.langmuir.6b02803
Langmuir 2016, 32, 10368−10376

$$S_{GCMC} = \frac{\left(\frac{q_{CO2}}{p_{CO2}}\right)}{\left(\frac{q_{H2O}}{p_{H2O}}\right)} \quad (3)$$

where q_i is the uptake of species i in mol/kg, and p_i is the partial pressure of species i in Pa.

Henry's law constants of CO_2, N_2, and H_2O for all CoRE MOFs were computed at 298 K using the Widom particle insertion method.[47] For Henry's law constant calculations, 100 000 configurational-biased insertions were performed throughout the simulation cell, and the Boltzmann-weighted framework-adsorbate interaction energies obtained from the random insertions were used to obtain the Henry's law constants. To break down the relative importance of van der Waals and Coulombic interactions to the adsorption energy, we carried out energy minimizations of a single adsorbate molecule inside the selected MOFs. From this, the minimum host-adsorbate energy among 100 independent minimizations via Baker's method[48] was chosen for further analysis of the van der Waals and Coulombic contributions to the adsorption energy between MOF and adsorbate molecule. A maximum of 10^4 minimization steps with the stopping criterion of RMS gradient of 1×10^{-6} were used. All simulations, including GCMC, Widom particle insertion calculations, and energy minimizations, were carried out using the RASPA simulation code.[49]

3. RESULTS AND DISCUSSION

High-Throughput Computational Screening. Because of the high-computational time associated with computing partial atomic charges from DFT (e.g., with REPEAT), we computed the Henry's law constants of CO_2, N_2, and H_2O for the CoRE MOFs using partial atomic charges derived from the EQeq method. Figure 2 shows the CO_2/H_2O selectivity based on the Henry's law constants versus the largest cavity diameter (LCD) of the MOFs. The initial screening suggests that MOFs with small pore size (<10 Å) tend to be more selective (S > 100) than MOFs with large pores (>10 Å). One notable exception is a MOF based on Zr_6-nodes known as PIZOF-1 (CSD REFCODE: OXOLAP), which shows high CO_2 selectivity and also a large LCD.[50]

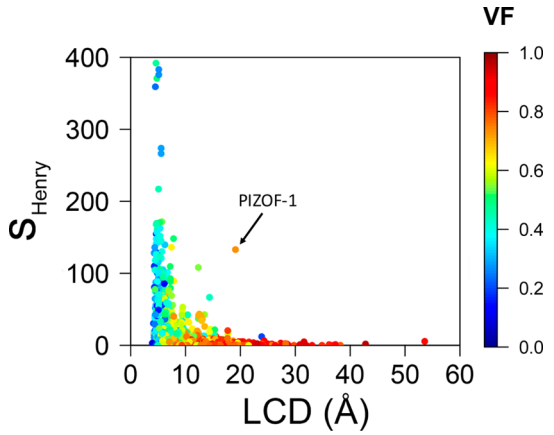

Figure 2. CO_2/H_2O selectivity based on the ratio of Henry's law constants between CO_2 and H_2O (S_{Henry}) against the largest cavity diameter (LCD) for 2054 CoRE MOFs. Data points are colored based on the void fraction (VF) of the structure.

On the basis of the ratio of Henry's law constants between CO_2 and H_2O, we chose the top 15 MOFs and carried out binary (CO_2/H_2O) and ternary ($CO_2/H_2O/N_2$) GCMC simulations with partial atomic charges obtained from the REPEAT method. GCMC simulations for a ternary mixture ($CO_2/H_2O/N_2$) were carried out under the postcombustion CO_2 capture conditions (1 bar and 298 K) with the relevant composition of the gas mixture (CO_2/N_2 = 1:9 and the relative humidity = 80%). Table 1 summarizes the physical properties of the selected MOFs for this study. We find that the MOFs with high CO_2/H_2O selectivity have small pores (4.5−5.7 Å) and relatively low void fractions.

Figure 3a shows the comparison between the selectivity based on the ratio of Henry's law constants and the selectivity based on the CO_2 and H_2O uptake computed from ternary mixture GCMC simulation. For the comparison between selectivities at the infinite dilution limit (Henry's law regime) and at finite loadings from GCMC simulations, we multiplied the selectivity based on the Henry's law constants by a constant factor (0.339) to account for the partial pressure ratio between CO_2 (9672 Pa) and H_2O (3280 Pa). As shown in Figure 3a, in general the adsorption selectivity based on the ratio of Henry's law constants overestimates the selectivity from the ternary GCMC simulations. Some disagreement is expected because the Henry's law constant only accounts for the interactions between MOF and adsorbate at low pressure and not the interactions among adsorbates, which can become more dominant at the pressure condition of interest.

The presence of N_2 could also affect the adsorption properties of CO_2 and H_2O as N_2 could compete for the binding sites within MOFs. We investigated the impact of N_2 on the adsorption of CO_2 and H_2O by comparing the CO_2/H_2O selectivity obtained from binary GCMC simulations with the CO_2/H_2O selectivity from ternary GCMC simulations. Figure 3b shows this comparison, and the results show that the CO_2/H_2O selectivity for the materials that we investigated here is insensitive to the presence of N_2. As noted in Table 1, these top-performing CoRE MOFs also exhibit high CO_2/N_2 selectivity, which shows that the selected CoRE MOFs are highly selective toward CO_2 in the presence of both H_2O and N_2.

A comparison of the selectivity rankings of the selected MOF structures based on Henry's law constants versus that from GCMC uptake is shown in Table 2. The results show that the ranking of adsorbents based on the ratio of Henry's law constants does a reasonably good job at correctly predicting top-performing MOFs from a set of structures. The top two structures predicted from the ratio of Henry's law constants (with the partial atomic charges obtained from REPEAT) are also the top two from the GCMC simulation (with the same partial atomic charges obtained from REPEAT). Most of the selected candidates exhibit high CO_2/H_2O selectivity, although IWELOM preferentially adsorbs H_2O over CO_2 (S_{GCMC} < 1). The results present the possibility of false-positive candidates from the screening based on the ratio of Henry's law constants of adsorbates. An important question is whether the ranking based on the Henry's law constants with REPEAT charges agrees with the ranking obtained from the GCMC simulations (with REPEAT charges), and our results tabulated in Table 2 show that the rankings are qualitatively similar. The Spearman rank correlation coefficient (ρ), a measure of the relationship between two independent ranking lists, was used to quantify how well the rankings in Table 2 agree with one another. If one ranking tends to increase when the other increases, the Spearman rank correlation coefficient ($-1 \leq \rho \leq +1$) is positive, and the higher the value of ρ, the closer the two rankings. When two rankings show perfect correlation, ρ becomes one. If one ranking decreases while the other ranking

DOI: 10.1021/acs.langmuir.6b02803
Langmuir 2016, 32, 10368−10376

Table 1. Physical Properties of the 15 Top Performing CoRE MOFs from Initial Screening[a]

REFCODE	VF	LCD (Å)	calc. surface area (m^2/g)	exp. surface area (m^2/g)	CO_2/H_2O selectivity (GCMC)	CO_2/N_2 selectivity (GCMC)
ZERQOE	0.25	4.5	315	*b*	80	78
PARMIG	0.5	4.6	717	*b*	53	57
HAWZEM	0.47	4.8	951	*b*	43	53
MUVGUG	0.52	5.3	1488	*c*	28	56
LIDZOP	0.3	5.6	389	*b*	27	84
MABLAD	0.36	5.3	901	*b*	25	126
MIMVEJ	0.47	4.7	808	*b*	17	35
KAXQIL	0.28	5.1	358	145	14	82
LIDZUV	0.28	5.1	348	224	12	81
LEZZEX	0.3	5.6	393	79	12	80
PEWXUL01	0.41	5.5	1183	*c*	8	79
EMIVAY	0.39	4.9	825	*b*	7	162
ITAHEQ	0.09	4.7	241	*d*	3	104
VICDOC	0.45	4.6	1044	1230	3	188
IWELOM	0.37	4.8	341	*b*	0.04	37

[a]Except VF (helium void fraction) obtained from RASPA,[49] all other structure properties were obtained from the Zeo++ software.[51,52] LCD is the largest cavity diameter, and REFCODE is the reference code from the Cambridge Structural Database (CSD). Selectivities are based on the results from ternary GCMC simulations. [b]The original paper does not report the experimental surface area of the MOF. [c]The original paper reports sorption data of other guest molecules but does not report a surface area. [d]Structure from private communication to CCDC. These structures are not published but deposited directly to CCDC.

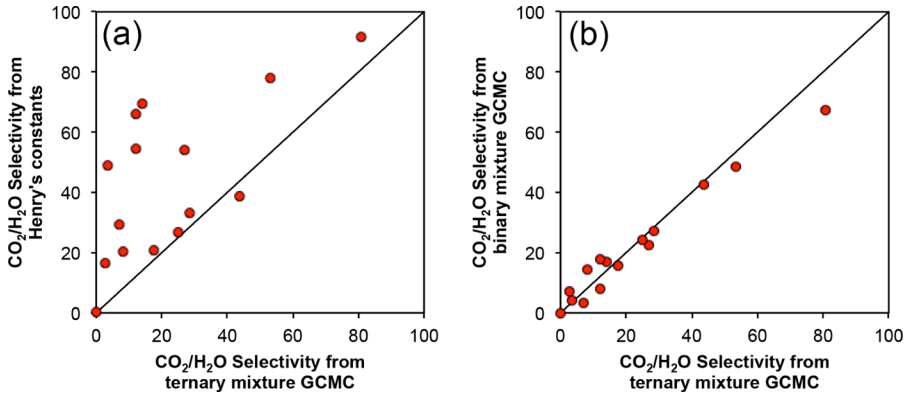

Figure 3. Comparison between the selectivity from different methods: (a) CO_2/H_2O selectivity obtained from the ratio of Henry's law constants for CO_2 and H_2O versus the CO_2/H_2O selectivity calculated for a ternary mixture of $CO_2/H_2O/N_2$ (CO_2/N_2 = 1:9 at RH = 80%) from GCMC simulation at 1 bar and 298 K; (b) CO_2/H_2O selectivity for a binary mixture of CO_2/H_2O (CO_2/H_2O = 7:2 at RH = 80%) at 0.15 bar and 298 K from GCMC simulation as a function of CO_2/H_2O selectivity for a ternary mixture of $CO_2/H_2O/N_2$ (CO_2/N_2 = 1:9, at RH = 80%) at 1 bar and 298 K from GCMC simulation. All of the results were obtained from simulations using REPEAT charges.

increases, ρ is negative. The Spearman correlation coefficient between K_H (REPEAT) and GCMC (REPEAT) is 0.61, slightly lower than that between K_H (EQeq) and K_H (REPEAT) (ρ = 0.76) but this result nonetheless indicates that the ratio of Henry's law constants could be used in identifying MOFs that preferentially adsorb CO_2 over H_2O under high humidity conditions.

In order to investigate the adsorption mechanism of the highly selective MOF candidates, GCMC simulations were carried out for the full range of pressures (0.1−1 bar) to compute the adsorption isotherms of CO_2, N_2, and H_2O for the top three candidates (CSD REFCODEs: ZERQOE,[53] PARMIG,[54] HAWZEM[55]). Figure 4 shows that the selected MOFs exhibit high CO_2 uptake, low N_2 uptake, and no H_2O uptake at a pressure above 0.2 bar. Notice that, below 0.2 bar, water molecules adsorb inside ZERQOE and PARMIG, but HAWZEM does not adsorb water, which suggests that HAWZEM is more hydrophobic than ZERQOE and PARMIG. In this work, we were looking for adsorbent materials that are selective toward CO_2 over H_2O but also have high capacity for CO_2 at the operating conditions. In this aspect, PARMIG and HAWZEM are better choices, because these MOFs adsorb more CO_2 than ZERQOE. ZERQOE shows the highest CO_2/H_2O selectivity (~80 at 1 bar and 298 K). Figure 4b shows representative snapshots from the simulations at 1 bar. It can be seen that the pores are fully filled and adsorbed CO_2 and N_2 molecules are generally clustered in the center of the very narrow pores.

Another MOF that we considered for detailed study is VICDOC,[56] which has the highest experimental surface area among the 15 MOFs from the initial screening. VICDOC has triangular-shaped one-dimensional channels and has been proposed in the literature for its excellent hydrocarbon isomer selectivity and capacity due to the strong confinement provided by the triangular shaped channels. As shown in Figure 5a, GCMC simulation results show that VICDOC exhibits high CO_2 uptake, low N_2 uptake, and decreased H_2O uptake at pressures above 0.5 bar. It appears from the snapshots in Figure 5b,c and the adsorption isotherm that more water molecules can fit inside the MOF channels than CO_2, and water molecules

DOI: 10.1021/acs.langmuir.6b02803
Langmuir 2016, 32, 10368−10376

Table 2. Ranking Based on CO_2/H_2O Selectivity Obtained from Henry's Law Constants with EQeq and REPEAT Charges and from GCMC Simulations of $CO_2/H_2O/N_2$ at 1 bar and 298 K with CO_2/N_2 = 1:9 and RH = 80%

MOF	K_H (EQeq)	K_H (REPEAT)	GCMC (REPEAT)
ZERQOE	4	1	1
PARMIG	1	2	2
HAWZEM	12	8	3
MUVGUG	7	9	4
LIDZOP	6	6	5
MABLAD	10	11	6
MIMVEJ	8	12	7
KAXQIL	3	3	8
LIDZUV	2	4	9
LEZZEX	5	5	10
PEWXUL01	15	13	11
EMIVAY	11	10	12
ITAHEQ	14	7	13
VICDOC	9	14	14
IWELOM	13	15	15

at 0.1 bar are more clustered together than the CO_2 molecules at 1 bar, which are spread more uniformly throughout the pore volume. The partial pressure of H_2O (3280 Pa) is much higher than that of CO_2 (672 Pa) at low total pressure (such as 0.1 bar); thus the pores are filled by H_2O molecules at these conditions. With increasing total pressure, CO_2 and H_2O in the mixture exhibit comparable partial pressures (e.g., P_{CO2} = 3270 Pa and P_{H2O} = 3280 Pa at 0.4 bar). Because of the stronger affinity of VICDOC toward CO_2 (K_H(REPEAT) = 2×10^{-3} mol kg^{-1} Pa^{-1}) than H_2O (K_H(REPEAT) = 4.2×10^{-5} mol kg^{-1} Pa^{-1}), more CO_2 molecules are adsorbed when the partial pressures are comparable.

Role of the Charge Calculation Method. The computed adsorption strength between polar molecules (e.g., H_2O) and MOF atoms depends on the method chosen for calculating or assigning partial atomic charges. There are a number of different methods available, such as Qeq,[57] EQeq,[30] DDEC,[58] ChelpG,[59] and REPEAT[39] and among these, the REPEAT method is a popular choice for periodic MOFs. However, the REPEAT method is time-consuming, which makes it difficult to apply for a large number of structures. As an alternative, the EQeq method can be used to rapidly assign point charges on MOFs as a first approximation prior to more expensive quantum calculations for top-performing structures. For the CoRE MOFs, reliable partial atomic charges from quantum mechanical calculations have been reported very recently (as this work was being finished) for 2932 of the CoRE MOFs,[60] but reliable charges are not yet available for the full set of structures. For instance, CoRE MOFs with large unit cells were not considered by Nazarian et al.[60] because these structures exceeded the maximum virtual memory imposed by the computing resources. Future work is needed in this direction to compute and assign DFT-derived partial charges to these structures. Nevertheless, we estimated the partial atomic charges from EQeq and REPEAT as a first pass of the screening. The EQeq method is faster than the quantum mechanical REPEAT method and also reasonably accurate because the dielectric strength and an electron affinity for hydrogen atoms used in EQeq were optimized to best fit REPEAT charges over a small set of MOF structures.[30] Recently, partial atomic charges based on EQeq have been used to discover hydrophobic MOFs from a very large database of hypothetical MOFs.[19]

To find out how the different methods used to calculate atomic partial charges of MOFs can affect the Henry's law constants of various adsorbates, we compared the Henry's constants obtained for the top 15 CoRE MOFs with different charge methods (EQeq and REPEAT) for CO_2, H_2O, and N_2 (Figure 6). The difference between EQeq and REPEAT is very

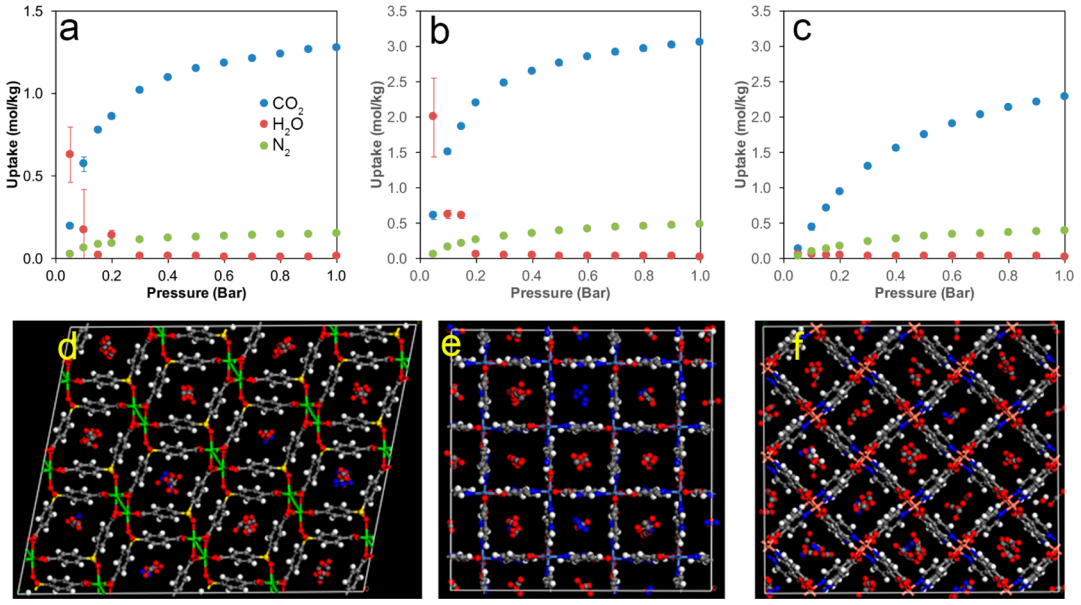

Figure 4. CO_2, H_2O, and N_2 isotherms of top-performing CoRE MOFs with REPEAT partial atomic charges for a ternary mixture of $CO_2/H_2O/N_2$ at 298 K with the molar ratio of CO_2/N_2 = 1:9 under RH at 80% (i.e., the partial pressure of H_2O is fixed at 3280 Pa throughout the entire pressure range): (a) ZERQOE, (b) PARMIG, and (c) HAWZEM; (d–f) snapshots from the simulation at p_{total} = 1 bar. The frameworks are represented in lines and the adsorbates are represented by Licorice, in which blue denotes nitrogen, white denotes hydrogen, red denotes oxygen, and gray denotes carbon, green denotes calcium, yellow denotes sulfur, light blue denotes nickel, and orange denotes copper.

DOI: 10.1021/acs.langmuir.6b02803
Langmuir 2016, 32, 10368–10376

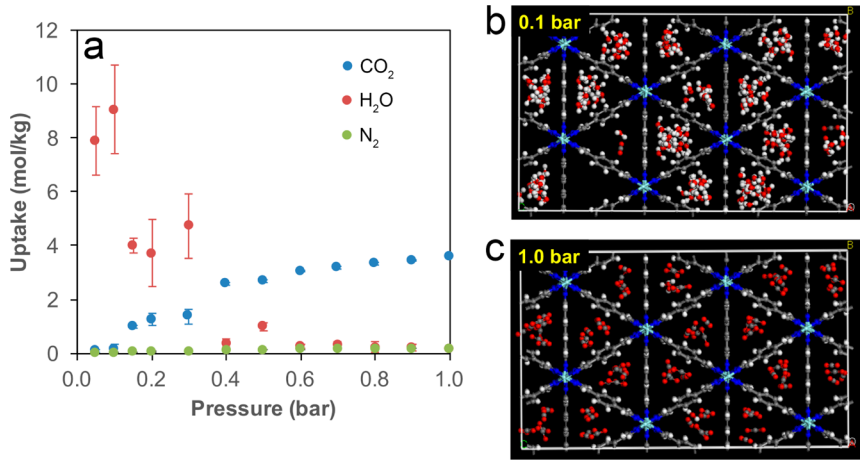

Figure 5. (a) CO_2, H_2O, and N_2 ternary mixture isotherm of VICDOC with REPEAT partial atomic charges at 298 K with the molar ratio of CO_2/N_2 = 1:9 under RH at 80% (i.e., the partial pressure of H_2O is fixed at 3280 Pa throughout the entire pressure range); (b) snapshot from ternary mixture GCMC simulation at 0.1 bar; (c) snapshot from ternary mixture GCMC simulation at 1 bar.

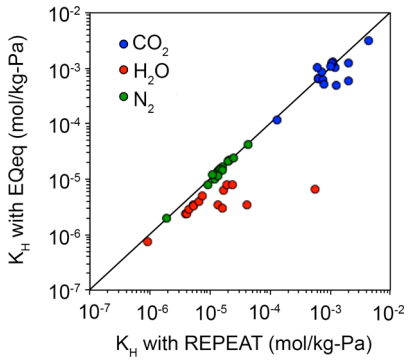

Figure 6. Comparison of the Henry's law constants (K_H) of CO_2, H_2O, and N_2 calculated from Widom insertions using the partial atomic charges based on EQeq method (*y*-axis) and REPEAT method (*x*-axis) at 298 K for the MOFs listed in Table 2.

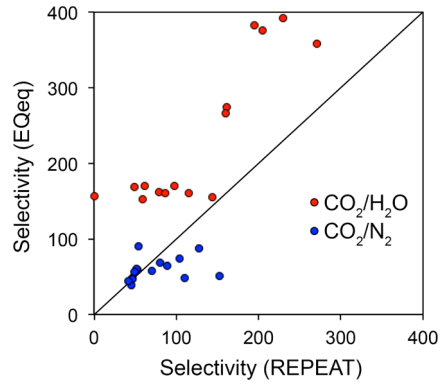

Figure 7. Comparison between the selectivities based on the ratio of Henry's law constants obtained for the structures with EQeq partial atomic charges (*y*-axis) and obtained for the structures with REPEAT partial atomic charges (*x*-axis). Red data points are for the selectivity between CO_2 and H_2O, and blue data points are the selectivity between CO_2 and N_2.

small for the Henry's law constants of N_2 and fairly small for CO_2. However, the Henry's law constant of H_2O is more sensitive to the choice of estimating the partial atomic charges. Notably, we find that EQeq systematically underestimates the interaction strength between H_2O and MOF atoms for the structures that we investigated here.

Figure 7 shows a comparison between the selectivity based on the ratio of Henry's law constants of different adsorbates for EQeq and REPEAT methods. Results are shown for both CO_2/H_2O selectivity and CO_2/N_2 selectivity. In terms of ranking the adsorbents for the separation, we find that the CO_2/H_2O selectivity rankings are not very sensitive to the choice of methods by which the partial atomic charges are assigned. The Spearman rank correlation coefficient between the rankings of K_H(EQeq) and K_H(REPEAT) is 0.76, suggesting the general agreement of the rankings from Henry's law constant estimation using different charge methods.

The relative contributions of electrostatic and van der Waals (vdW) interactions to the adsorption energy of CO_2, H_2O, and N_2 within the 15 MOFs are shown in Figure 8. Overall, there is a stronger binding between MOF and CO_2 than between MOF and N_2 or H_2O for these MOFs. For CO_2 and N_2, the adsorption energy is dominated by van der Waals interactions. Coulombic interactions play a more dominant role in the adsorption of H_2O, where the electrostatic contribution to the total adsorption energy is comparable or even larger than the van der Waals contribution. The results demonstrate that H_2O adsorption energies can be sensitive to the methods used to approximate the partial atomic charges in the MOF, suggesting the importance of developing accurate, but fast, charge calculation methods.

4. CONCLUSION

We present a high-throughput computational strategy to find suitable candidate MOFs from the CoRE MOF database that can effectively adsorb CO_2 at 80% relative humidity during postcombustion CO_2 capture. We first identified MOFs with high CO_2/H_2O selectivities based on the ratio of Henry's law constants of CO_2 and H_2O. The adsorption characteristics of the top MOFs were then computed using GCMC simulations under postcombustion CO_2 capture conditions. Ternary mixture simulations of selected top-performing MOFs show that our strategy works reasonably well to find MOFs with high CO_2/H_2O and CO_2/N_2 selectivities. We also find that the electrostatic interactions play an important role in describing the interaction between H_2O and MOF, which suggests that accurate charge calculation methods must be used to simulate

DOI: 10.1021/acs.langmuir.6b02803
Langmuir 2016, 32, 10368−10376

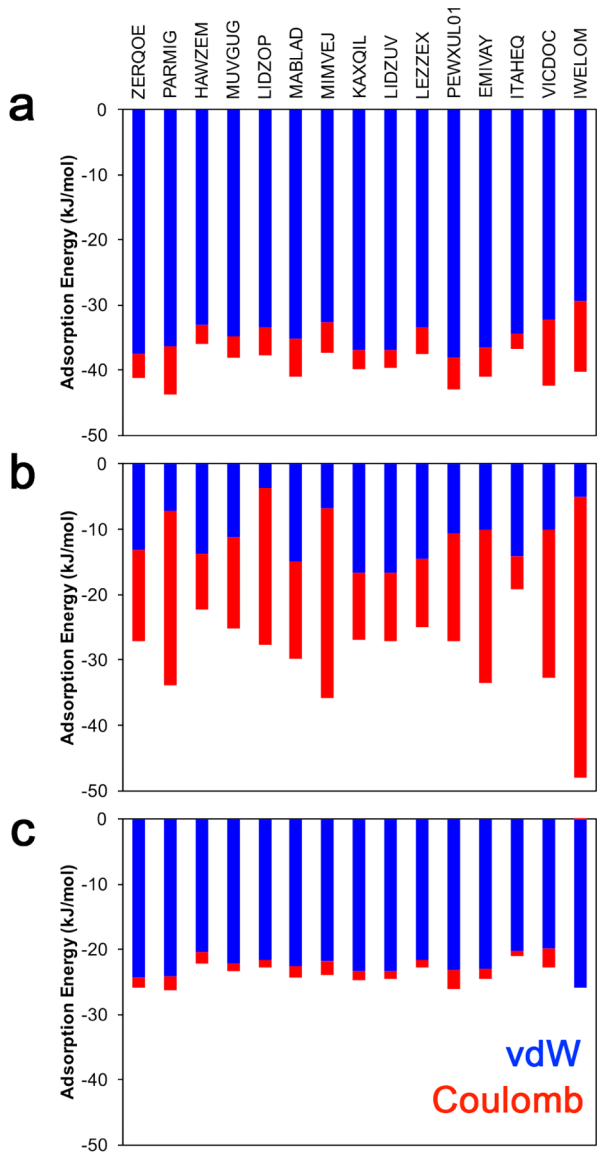

Figure 8. Adsorption energy between (a) MOF-CO_2, (b) MOF-H_2O, and (c) MOF-N_2 for selected 15 MOFs in the order from Table 2 (left to right). Adsorption energies are calculated from energy minimization of a single adsorbate molecule inside the MOF with REPEAT charges.

H_2O in MOFs. We find that the use of the EQeq method to calculate the Henry's law constants of H_2O can lead to significant underestimation of the Henry's law constants when compared to calculations using charges from the REPEAT method from plane-wave DFT calculations. The underestimation of Henry's law constants for H_2O leads to overestimation of the CO_2/H_2O selectivity. Our results further show that high CO_2/H_2O selectivity originates from strong van der Waals interaction between pore walls and CO_2 molecules, and the adsorption energies of CO_2 within these selected MOFs show that the van der Waals interaction between CO_2 and MOF atoms is more important than the electrostatic interaction. Development of high-performing MOFs for industrial CO_2 capture at high humidity is a great challenge. According to this work, small pore size provides strong binding of CO_2 and limits water uptake at high humidity by preventing the formation of water clusters inside the pores. However, MOFs with small pore sizes may have lower working capacity compared to other adsorbent materials with larger pore volumes, and future work is needed in developing and designing hydrophobic MOFs with high CO_2 working capacity.

AUTHOR INFORMATION

Notes

The authors declare the following competing financial interest(s): Randall Snurr has a financial interest in the start-up company NuMat Technologies, which is seeking to commercialize metal-organic frameworks.

ACKNOWLEDGMENTS

This work was supported by the U.S. Department of Energy, Office of Basic Energy Sciences, Division of Chemical Sciences, Geosciences and Biosciences, under Award DE-FG02-12ER16362. We thank the National Energy Research Scientific Computing Center (NERSC), which is supported by the Office of Science of the U.S. Department of Energy under Contract No. DE-AC02-05CH11231, for computational resources, and the computational resources and staff contributions provided by the Quest high-performance computing facility at Northwestern University (p20663), which is jointly supported by the Office of the Provost, the Office for Research, and Northwestern University Information Technology.

REFERENCES

(1) Feldman, D. R.; Collins, W. D.; Gero, P. J.; Torn, M. S.; Mlawer, E. J.; Shippert, T. R. Observational Determination of Surface Radiative Forcing by CO_2 from 2000 to 2010. *Nature* **2015**, *519*, 339−343.

(2) *Inventory of U.S. Greenhouse Gas Emissions and Sinks: 1990−2006*; Environmental Protection Agency, Washington, DC, 2008.

(3) Yang, H.; Xu, Z.; Fan, M.; Gupta, R.; Slimane, R. B.; Bland, A. E.; Wright, I. Progress in Carbon Dioxide Separation and Capture: A Review. *J. Environ. Sci.* **2008**, *20*, 14−27.

(4) D'Alessandro, D. M.; Smit, B.; Long, J. R. Carbon Dioxide Capture: Prospects for New Materials. *Angew. Chem., Int. Ed.* **2010**, *49*, 6058−6082.

(5) Sumida, K.; Rogow, D. L.; Mason, J. A.; McDonald, T. M.; Bloch, E. D.; Herm, Z. R.; Bae, T.-H.; Long, J. R. Carbon Dioxide Capture in Metal-Organic Frameworks. *Chem. Rev.* **2012**, *112*, 724−781.

(6) Liu, J.; Thallapally, P. K.; McGrail, B. P.; Brown, D. R.; Liu, J. Progress in Adsorption-Based CO_2 Capture by Metal-Organic Frameworks. *Chem. Soc. Rev.* **2012**, *41*, 2308−2322.

(7) Long, J. R.; Yaghi, O. M. The Pervasive Chemistry of Metal-Organic Frameworks. *Chem. Soc. Rev.* **2009**, *38*, 1213−1214.

(8) Eddaoudi, M.; Moler, D. B.; Li, H.; Chen, B.; Reineke, T. M.; O'Keeffe, M.; Yaghi, O. M. Modular Chemistry: Secondary Building Units as a Basis for the Design of Highly Porous and Robust Metal-Organic Carboxylate Frameworks. *Acc. Chem. Res.* **2001**, *34*, 319−330.

(9) Ferey, G. Hybrid Porous Solids: Past, Present, Future. *Chem. Soc. Rev.* **2008**, *37*, 191−214.

(10) Yazaydın, A. Ö.; Snurr, R. Q.; Park, T.-H.; Koh, K.; Liu, J.; LeVan, M. D.; Benin, A. I.; Jakubczak, P.; Lanuza, M.; Galloway, D. B.; Low, J. J.; Willis, R. R. Screening of Metal-Organic Frameworks for Carbon Dioxide Capture from Flue Gas Using a Combined Experimental and Modeling Approach. *J. Am. Chem. Soc.* **2009**, *131*, 18198−18199.

(11) Choi, S.; Drese, J. H.; Jones, C. W. Adsorbent Materials for Carbon Dioxide Capture from Large Anthropogenic Point Sources. *ChemSusChem* **2009**, *2*, 796−854.

(12) Bae, Y. S.; Snurr, R. Q. Development and Evaluation of Porous Materials for Carbon Dioxide Separation and Capture. *Angew. Chem., Int. Ed.* **2011**, *50*, 11586−11596.

(13) McDonald, T. M.; Mason, J. A.; Kong, X. Q.; Bloch, E. D.; Gygi, D.; Dani, A.; Crocella, V.; Giordanino, F.; Odoh, S. O.; Drisdell, W. S.; Vlaisavljevich, B.; Dzubak, A. L.; Poloni, R.; Schnell, S. K.; Planas, N.;

DOI: 10.1021/acs.langmuir.6b02803
Langmuir 2016, 32, 10368−10376

Lee, K.; Pascal, T.; Wan, L. W. F.; Prendergast, D.; Neaton, J. B.; Smit, B.; Kortright, J. B.; Gagliardi, L.; Bordiga, S.; Reimer, J. A.; Long, J. R. Cooperative Insertion of CO_2 in Diamine-Appended Metal-Organic Frameworks. *Nature* **2015**, *519*, 303−308.
(14) Liu, J.; Benin, A. I.; Furtado, A. M. B.; Jakubczak, P.; Willis, R. R.; LeVan, M. D. Stability Effects on CO_2 Adsorption for the Dobdc Series of Metal-Organic Frameworks. *Langmuir* **2011**, *27*, 11451−11456.
(15) Kizzie, A. C.; Wong-Foy, A. G.; Matzger, A. J. Effect of Humidity on the Performance of Microporous Coordination Polymers as Adsorbents for CO_2 Capture. *Langmuir* **2011**, *27*, 6368−6373.
(16) Keskin, S.; van Heest, T. M.; Sholl, D. S. Can Metal−Organic Framework Materials Play a Useful Role in Large-Scale Carbon Dioxide Separations? *ChemSusChem* **2010**, *3*, 879−891.
(17) Furukawa, H.; Gandara, F.; Zhang, Y.-B.; Jiang, J.; Queen, W. L.; Hudson, M. R.; Yaghi, O. M. Water Adsorption in Porous Metal-Organic Frameworks and Related Materials. *J. Am. Chem. Soc.* **2014**, *136*, 4369−4381.
(18) Burtch, N. C.; Jasuja, H.; Walton, K. S. Water Stability and Adsorption in Metal-Organic Frameworks. *Chem. Rev.* **2014**, *114*, 10575−10612.
(19) Moghadam, P. Z.; Fairen-Jimenez, D.; Snurr, R. Q. Efficient Identification of Hydrophobic MOFs: Application in the Capture of Toxic Industrial Chemicals. *J. Mater. Chem. A* **2016**, *4*, 529−536.
(20) Leperi, K. T.; Snurr, R. Q.; You, F. Optimization of Two-Stage Pressure/Vacuum Swing Adsorption with Variable Dehydration Level for Postcombustion Carbon Capture. *Ind. Eng. Chem. Res.* **2016**, *55*, 3338−3350.
(21) Colon, Y. J.; Snurr, R. Q. High-Throughput Computational Screening of Metal-Organic Frameworks. *Chem. Soc. Rev.* **2014**, *43*, 5735−5749.
(22) Colon, Y. J.; Fairen-Jimenez, D.; Wilmer, C. E.; Snurr, R. Q. High-Throughput Screening of Porous Crystalline Materials for Hydrogen Storage Capacity near Room Temperature. *J. Phys. Chem. C* **2014**, *118*, 5383−5389.
(23) Goldsmith, J.; Wong-Foy, A. G.; Cafarella, M. J.; Siegel, D. J. Theoretical Limits of Hydrogen Storage in Metal-Organic Frameworks: Opportunities and Trade-Offs. *Chem. Mater.* **2013**, *25*, 3373−3382.
(24) Simon, C. M.; Mercado, R.; Schnell, S. K.; Smit, B.; Haranczyk, M. What Are the Best Materials to Separate a Xenon/Krypton Mixture? *Chem. Mater.* **2015**, *27*, 4459−4475.
(25) Bai, P.; Jeon, M. Y.; Ren, L. M.; Knight, C.; Deem, M. W.; Tsapatsis, M.; Siepmann, J. I. Discovery of Optimal Zeolites for Challenging Separations and Chemical Transformations Using Predictive Materials Modeling. *Nat. Commun.* **2015**, *6*, 5912.
(26) Wilmer, C. E.; Leaf, M.; Lee, C. Y.; Farha, O. K.; Hauser, B. G.; Hupp, J. T.; Snurr, R. Q. Large-Scale Screening of Hypothetical Metal-Organic Frameworks. *Nat. Chem.* **2011**, *4*, 83−89.
(27) Fernandez, M.; Boyd, P. G.; Daff, T. D.; Aghaji, M. Z.; Woo, T. K. Rapid and Accurate Machine Learning Recognition of High Performing Metal Organic Frameworks for CO_2 Capture. *J. Phys. Chem. Lett.* **2014**, *5*, 3056−3060.
(28) Wilmer, C. E.; Farha, O. K.; Bae, Y. S.; Hupp, J. T.; Snurr, R. Q. Structure-Property Relationships of Porous Materials for Carbon Dioxide Separation and Capture. *Energy Environ. Sci.* **2012**, *5*, 9849−9856.
(29) Chung, Y. G.; Camp, J.; Haranczyk, M.; Sikora, B. J.; Bury, W.; Krungleviciute, V.; Yildirim, T.; Farha, O. K.; Sholl, D. S.; Snurr, R. Q. Computation-Ready, Experimental Metal-Organic Frameworks: A Tool to Enable High-Throughput Screening of Nanoporous Crystals. *Chem. Mater.* **2014**, *26*, 6185−6192.
(30) Wilmer, C. E.; Kim, K. C.; Snurr, R. Q. An Extended Charge Equilibration Method. *J. Phys. Chem. Lett.* **2012**, *3*, 2506−2511.
(31) Haldoupis, E.; Nair, S.; Sholl, D. S. Finding MOFs for Highly Selective CO_2/N_2 Adsorption Using Materials Screening Based on Efficient Assignment of Atomic Point Charges. *J. Am. Chem. Soc.* **2012**, *134*, 4313−4323.
(32) Watanabe, T.; Sholl, D. S. Accelerating Applications of Metal-Organic Frameworks for Gas Adsorption and Separation by Computational Screening of Materials. *Langmuir* **2012**, *28*, 14114−14128.
(33) Rappe, A. K.; Casewit, C. J.; Colwell, K. S.; Goddard, W. A.; Skiff, W. M. UFF, a Full Periodic-Table Force-Field for Molecular Mechanics and Molecular-Dynamics Simulations. *J. Am. Chem. Soc.* **1992**, *114*, 10024−10035.
(34) McDaniel, J. G.; Li, S.; Tylianakis, E.; Snurr, R. Q.; Schmidt, J. R. Evaluation of Force Field Performance for High-Throughput Screening of Gas Uptake in Metal-Organic Frameworks. *J. Phys. Chem. C* **2015**, *119*, 3143−3152.
(35) Potoff, J. J.; Siepmann, J. I. Vapor-Liquid Equilibria of Mixtures Containing Alkanes, Carbon Dioxide, and Nitrogen. *AIChE J.* **2001**, *47*, 1676−1682.
(36) Jorgensen, W. L.; Chandrasekhar, J.; Madura, J. D.; Impey, R. W.; Klein, M. L. Comparison of Simple Potential Functions for Simulating Liquid Water. *J. Chem. Phys.* **1983**, *79*, 926−935.
(37) Ghosh, P.; Kim, K. C.; Snurr, R. Q. Modeling Water and Ammonia Adsorption in Hydrophobic Metal-Organic Frameworks: Single Components and Mixtures. *J. Phys. Chem. C* **2014**, *118*, 1102−1110.
(38) Ewald, P. P. Die Berechnung Optischer Und Elektrostatischer Gitterpotentiale. *Ann. Phys.* **1921**, *369*, 253−287.
(39) Campana, C.; Mussard, B.; Woo, T. K. Electrostatic Potential Derived Atomic Charges for Periodic Systems Using a Modified Error Functional. *J. Chem. Theory Comput.* **2009**, *5*, 2866−2878.
(40) Kresse, G.; Furthmuller, J. Efficiency of Ab-Initio Total Energy Calculations for Metals and Semiconductors Using a Plane-Wave Basis Set. *Comput. Mater. Sci.* **1996**, *6*, 15−50.
(41) Kresse, G.; Furthmüller, J. Efficient Iterative Schemes for Ab Initio Total-Energy Calculations Using a Plane-Wave Basis Set. *Phys. Rev. B: Condens. Matter Mater. Phys.* **1996**, *54*, 11169−11186.
(42) Kresse, G.; Hafner, J. Ab Initio Molecular Dynamics for Liquid Metals. *Phys. Rev. B: Condens. Matter Mater. Phys.* **1993**, *47*, 558−561.
(43) Kresse, G.; Hafner, J. Ab Initio Molecular-Dynamics Simulation of the Liquid-Metal-Amorphous-Semiconductor Transition in Germanium. *Phys. Rev. B: Condens. Matter Mater. Phys.* **1994**, *49*, 14251−14269.
(44) Perdew, J. P.; Burke, K.; Ernzerhof, M. Generalized Gradient Approximation Made Simple. *Phys. Rev. Lett.* **1996**, *77*, 3865−3868.
(45) Norman, G. E.; Filinov, V. S. Investigations of Phase Transitions by a Monte-Carlo Method. *High Temp.* **1969**, *7*, 216.
(46) Vega, C.; Abascal, J. L. F.; Nezbeda, I. Vapor-Liquid Equilibria from the Triple Point up to the Critical Point for the New Generation of Tip4p-Like Models: Tip4p/Ew, Tip4p/2005, and Tip4p/Ice. *J. Chem. Phys.* **2006**, *125*, 034503.
(47) Widom, B. Some Topics in the Theory of Fluids. *J. Chem. Phys.* **1963**, *39*, 2808.
(48) Baker, J. An Algorithm for the Location of Transition States. *J. Comput. Chem.* **1986**, *7* (4), 385−395.
(49) Dubbeldam, D.; Calero, S.; Ellis, D. E.; Snurr, R. Q. RASPA: Molecular Simulation Software for Adsorption and Diffusion in Flexible Nanoporous Materials. *Mol. Simul.* **2016**, *42*, 81−101.
(50) Schaate, A.; Roy, P.; Preusse, T.; Lohmeier, S. J.; Godt, A.; Behrens, P. Porous Interpenetrated Zirconium-Organic Frameworks (Pizofs): A Chemically Versatile Family of Metal-Organic Frameworks. *Chem. - Eur. J.* **2011**, *17*, 9320−9325.
(51) Willems, T. F.; Rycroft, C. H.; Kazi, M.; Meza, J. C.; Haranczyk, M. Algorithms and Tools for High-Throughput Geometry- Based Analysis of Crystalline Porous Materials. *Microporous Mesoporous Mater.* **2012**, *149*, 134−141.
(52) Martin, R. L.; Smit, B.; Haranczyk, M. Addressing Challenges of Identifying Geometrically Diverse Sets of Crystalline Porous Materials. *J. Chem. Inf. Model.* **2012**, *52*, 308−318.
(53) Banerjee, D.; Zhang, Z. J.; Plonka, A. M.; Li, J.; Parise, J. B. A Calcium Coordination Framework Having Permanent Porosity and High CO_2/N_2 Selectivity. *Cryst. Growth Des.* **2012**, *12*, 2162−2165.

DOI: 10.1021/acs.langmuir.6b02803
Langmuir 2016, 32, 10368−10376

(54) Wu, L.; Xue, M.; Huang, L.; Qiu, S. L. Hydrothermal Synthesis, Structure, Fluorescence Property of a Novel 3d Metal-Organic Framework with High Thermal Stability. *Sci. China: Chem.* **2011**, *54*, 1441−1445.
(55) Lian, T. T.; Chen, S. M. A New Microporous Cu(II)-Isonicotinate Framework with 8-Connected Bcu Topology. *Inorg. Chem. Commun.* **2012**, *18*, 8−10.
(56) Herm, Z. R.; Wiers, B. M.; Mason, J. A.; van Baten, J. M.; Hudson, M. R.; Zajdel, P.; Brown, C. M.; Masciocchi, N.; Krishna, R.; Long, J. R. Separation of Hexane Isomers in a Metal-Organic Framework with Triangular Channels. *Science* **2013**, *340*, 960−964.
(57) Rappe, A. K.; Goddard, W. A. Charge Equilibration for Molecular-Dynamics Simulations. *J. Phys. Chem.* **1991**, *95*, 3358−3363.
(58) Manz, T. A.; Sholl, D. S. Chemically Meaningful Atomic Charges That Reproduce the Electrostatic Potential in Periodic and Nonperiodic Materials. *J. Chem. Theory Comput.* **2010**, *6*, 2455−2468.
(59) Breneman, C. M.; Wiberg, K. B. Determining Atom-Centered Monopoles from Molecular Electrostatic Potentials. The Need for High Sampling Density in Formamide Conformational Analysis. *J. Comput. Chem.* **1990**, *11*, 361−373.
(60) Nazarian, D.; Camp, J. S.; Sholl, D. S. A Comprehensive Set of High-Quality Point Charges for Simulations of Metal-Organic Frameworks. *Chem. Mater.* **2016**, *28*, 785−793.

DOI: 10.1021/acs.langmuir.6b02803
Langmuir 2016, 32, 10368−10376